Journal of Engineering Science and Technology Review 17 (4) (2024) 210-219

Research Article

JOURNAL OF
Engineering Science and Technology Review

www.jestr.org

Trajectory Tracking Control with Soft Switching based on Antislip Sliding Mode for High-clearance Mobile Robot

Na Wang[1,*], Erbao Peng[1], Chuansheng Tang[2], Chaojun Wang[3] and Jie Yang[4,5]

[1]*Henan Polytechnic Institute, Nanyang Henan 473000, China*
[2]*Chongqing City Vocational College, Chongqing 402160, China*
[3]*Zhengzhou Vocational University of Information and Technology, Zhengzhou Henan 450046, China*
[4]*Henan Institute of Technology, Xinxiang Henan 453000, China*
[5]*Department of Computer Engineering, Dongseo University, Busan 47011, South Korea*

Received 20 June 2024; Accepted 13 August 2024

Abstract

The trajectory tracking accuracy of high-clearance mobile robots could be affected by phenomena such as wheel slippage caused by changes in the working surface material and motion state. To reveal the impact of slippage factor and improve the tracking precision of wheeled mobile robots, this study proposed a sliding mode of trajectory tracking control with soft switching. Considering the slippage working environment of mobile robots, a three-degrees-of-freedom kinematic model of mobile robots containing slip rate was established. Based on the kinematic model of the system, a trajectory tracking controller utilizing soft switching sliding mode control was developed, followed by a comprehensive stability analysis. The MATLAB platform was utilized to verify the circular trajectory tracking performance of the mobile robot under both slipping and nonslipping conditions. Results demonstrate that: (1) Under ideal conditions (disregarding wheel slippage), the sliding mode tracker based on model design quickly achieves high-precision tracking of the robot's trajectory, with the tracking error controlled at 0.002 m within 0.6 s in a circular trajectory, capable of adjusting and tracking the desired circular trajectory in a short time and maintaining consistent posture. (2) When considering the effect of slippage, the uncompensated sliding mode control produces a larger periodic tracking error (the amplitude of the circular trajectory reaches 0.065 m) and a larger direction angle error at the trough of the lateral position, causing a sudden change in the direction angle. Nevertheless, the proposed sliding compensation in this study can improve its accuracy by about twice, with the tracking error controlled around 0.03 m in circular trajectories, effectively improving the system's tracking accuracy. This study expands the working environment of mobile robots and provides a basis for their high-performance operation in complex environments.

Keywords: Mobile robot, Kinematic model, Sliding mode trajectory, Soft switching, Tracking control, Three-degrees-of-freedom

1. Introduction

As computer and automation technology rapidly advances, and high-tech applications become widespread in agriculture, robotic technology is progressively being integrated into agricultural production. This integration is driving modern agriculture towards greater mechanization of equipment and the adoption of intelligent production methods. High-clearance robots have a high ground clearance, large pesticide tank capacity, and a high center of gravity of the whole machine. During the driving process, they are prone to dangerous situations such as overturning due to external excitation or extremely fast turning speed. Vehicle overturning primarily occurs due to significant lateral acceleration, which results in the lateral load shifting between the left and right sides of the vehicle. This shift can cause one side of the wheels to lift off the ground, leading to an overturn. The existing control of high-clearance mobile robots mainly designs the control system without considering the situation of wheels and the ground, lacking study in complex working environments [1, 2]. A team from the Hubei University of Technology [3] carried out a detailed design of a robot's walking mechanism and a longitudinal stability system but did not consider the dynamic characteristics of wheel slip on the ground. For a hydraulic-driven high-clearance spray robot, a team from Jiangsu University [4] introduced the slip rate and proposed a fuzzy antislip tracking control strategy but lacked a dynamic analysis of the system. The controller structure was complex, making it difficult to physically implement.

The high-clearance mobile robot working system is a complex and variable dynamic system. The wheel slip during its operation is affected by multiple factors, and an accurate and comprehensive wheel slip dynamic model is difficult to establish. In consideration of the main characteristics of vehicle overturning, a simplified slip dynamic model is established to ensure that it can accurately reflect the general slip characteristics and further improve the real-time performance of the entire slip model [5–9].

On the basis of the preceding analysis, this study evaluates the ground kinematic model of a high-clearance mobile robot under normal conditions, establishes a coupled motion state model of steering and longitudinal slip, and designs a unified sliding mode controller that could adapt to the needs of complex agricultural environments.

*E-mail address: hnjzwm@126.com
ISSN: 1791-2377
doi:10.25103/jestr.174.23

2. State of the art

Mobile robots regulate their velocity and directional orientation by adjusting the rotational speeds of their four independently actuated wheels. The control problem between the speed and position of a mobile robot can be solved through the kinematic model of the mobile robot [10]. An accurate kinematic model of the mobile robot is based on geometry to describe the motion laws of the mobile robot, enabling the mobile robot to quickly track the desired trajectory or planned path [11].

In response to the coupling issues of forward and steering speeds of wheeled mobile robots under unbalanced load conditions, Li et al. [12] proposed an active disturbance rejection control strategy for speed regulation based on a kinematic model with an antidisturbance proportional–integral–derivative (PID) controller. It had a certain antidisturbance effect on external disturbances, but the phenomenon of wheel slip was not considered in the system. In view of the interference of various waveform when mobile robots move in complex environments, Xu et al. [13] proposed an intelligent PID tracking control strategy for mobile robots. While the system demonstrated robust anti-interference capabilities and high tracking precision, its performance was predicated on the assumption of no wheel slippage. To tackle the speed tracking issue in nonholonomic wheeled mobile robots affected by external disturbances and measurement noise, Raza et al. [14] introduced a fractional-order PID controller that is derived from the robot's kinematic model, and the controller parameters were optimally adjusted using a combination algorithm. When wheel slip occurred, the system performance decreased, and it could even cause instability or accidents. Carlucho et al. [15] combined deep reinforcement learning with PID control and proposed an adaptive multi-PID intelligent controller for mobile robots based on deep reinforcement learning. Employing an actor–critic framework, the system ingested only low-level dynamic information as input for the purpose of estimating multiple parameters or gains of the PID controller. The system structure was complex and difficult to adapt to high-performance dynamic response. The above proposed methods were all based on PID, established under the premise that the system model was known and the structure was determined. They ignored the model uncertainty caused by wheel slip during the operation process of the mobile robot, thus hardly meeting the requirements of system accuracy.

For meeting the requirements of complex environments and making the system have strong robustness and anti-interference capabilities, various modern control methods, such as robust control, finite-time control, backstepping control, predictive control, and adaptive control, have become hot topics in the trajectory tracking control of mobile robots [16–23]. Zheng et al. [16] proposed an optimal robust control approach for mobile robots engaged in a cooperative game, taking into account that the trajectory tracking control performance of wheeled mobile robots is influenced by positional constraints, system uncertainties, and external disturbances. Although the proposed method had strong robustness and high tracking accuracy, it caused the system structure to be complex, and the model was based on an ideal situation without wheel slip. Colorado [17] introduced an observer-based finite-time control scheme for trajectory tracking of wheeled mobile robots that are subject to motion disturbances. Although the proposed method could achieve rapid tracking of trajectories, it did not consider the nonlinear dynamic relationship between the wheels and the ground in complex working environments. Ríos et al. [18] proposed a model predictive control method based on an interval predictor for the trajectory tracking problem of a unicycle mobile robot affected by disturbances. The proposed method's anti-interference ability and robustness were verified through a tracking simulation of double rings and circular curves, but model predictive control could reduce the system sampling frequency, affecting the system's real-time response ability. Hannes et al. [19] used Gaussian processes and model predictive control to achieve trajectory tracking of exploration mobile robots. The system performance had high tracking accuracy for an ideal nonslip situation but lacked study on slip conditions. Majid et al. [20] designed a model predictive trajectory tracking controller for mobile robots with differences between the center of mass and the geometric center. The feedforward control was directly calculated from the reference trajectory, and the feedback control was designed on the basis of a linearized tracking error model using model predictive control. The model was implemented without accounting for the nonlinear dynamics between the wheels and the ground in complex operational environments, failing to mitigate the impact of model inaccuracies on system performance. Zhang et al. [21] introduced an adaptive trajectory tracking control method for nonholonomic wheeled mobile robots with problems such as slipping, unknown external disturbances, model uncertainty, and input saturation constraints. A radial basis function neural network was utilized to address unknown external disturbances within robot dynamics, while a nonlinear disturbance observer was employed to estimate disturbances, including wheel slip and robot slip. The adaptive control scheme's efficacy was confirmed through simulation experiments. Although the proposed method effectively countered performance degradation due to slipping, the incorporation of neural networks increased system complexity, potentially impacting the system's response speed. To achieve efficient and robust autonomous mobile robot motion, Liu et al. [22] proposed a robust control scheme for wheeled mobile robots based on the control Lyapunov function. A robust controller based on the Lyapunov function was designed for structural uncertainty and slip disturbance in the robot kinematic model, and a quadratic programming of the controller was given. The proposed method regarded the robot as an idealized trajectory generator, often lacking consideration of the actual motion model of the robot. Shou et al. [23] combined a robot's kinematic and dynamic equations and obtained the virtual control value of the control speed via the Lyapunov method. The cerebellar model articulation controller (CMAC) was deployed to approximate the nonlinear characteristics and uncertainties inherent in the mobile robot's dynamic model. This proposed approach ensured global system stability and the asymptotic convergence of tracking errors. However, the tracking precision was influenced by the architecture of the CMAC network, and determining the optimal number of network layers and the weights posed a challenge. Chai et al. [24] used an improved backstepping method, introduced a saturation function for error compensation, and employed an optimization algorithm to achieve online tuning of the controller, achieving rapid and accurate convergence of trajectory tracking errors. The proposed method was based on a model under the premise of certainty, but the slippage in actual operation may cause overturning phenomena, which could cause system failure.

Park et al. [25] proposed a leader-following tracking control method for mobile robots. A machine learning approach grounded in physical insights was utilized for velocity estimation of the lead robot, with the dynamic traits of the state observer being learned via an error state model. The robust control techniques of the polyhedral model were applied to convexly combine the gains of the parameter-dependent tracking controller. The proposed method relied on a kinematic model assuming non-slip wheel conditions for control, yet it lacked empirical validation under real-world operational scenarios.

Intelligent control has the characteristic of fitting arbitrary nonlinear curves and has been widely concerned in the tracking control of mobile robots. Liu et al. [26] considered that an underactuated wheeled mobile robot system includes unknown nonlinear dynamics and used a fuzzy logic system to approximate the unknown nonlinear dynamics. The proposed method could ensure that the controlled mobile robot system had intermittent actuator faults, and the tracking error remained within the specified boundary. However, the error caused by the uncertainty of the model structure was difficult to improve. Onur [27] used a single-layer neural network to achieve automatic control of agricultural mobile robots, which was applied to online operations in farms and greenhouses. The operation had high tracking performance in an ideal environment, but when the ground was wet and caused wheel slip, the system performance was significantly reduced. Combining optimal control theory, adaptive neural network systems, and robust control technology, Boukens et al. [28] used neural network systems to approximate nonlinear functions in the optimal control law. The robust controller adaptively estimated the unknown upper bounds of time-varying parameter uncertainty, external disturbances, and approximation errors of the neural network systems. The controller exhibited high precision and dynamic responsiveness under the assumption that slip-induced overturning, a potential issue in real-world operations, was not considered. The aforementioned control strategies predominantly employed intelligent control techniques, including fuzzy logic and neural networks, to achieve disturbance rejection without the need for an exact disturbance analysis model. A common drawback of these methods was the dependence on empirical data and training; consequently, real-time and effective control was difficult to achieve when the actual environment was unstable and training was insufficient. Sliding mode control has strong robustness against model matching and external disturbances. Ovalle et al. [29] proposed a robust sliding mode position tracking control strategy for omnidirectional mobile robots when only the robot's position and direction information is available. The proposed method was designed on the basis of a known model structure and had strong robustness against model matching uncertainty and inherent chattering phenomena. To achieve precise tracking of high-speed motion of mobile robots on unknown slope terrain, Alihosseini et al. [30] proposed a robust nonlinear sliding mode control method. The proposed method exhibited good performance in specific environments, but in its system output, the chattering caused by the unmodeled dynamics of the control system was still difficult to suppress. This output chattering can have unpredictable effects on the robot operation in a real environment, thereby weakening the system's robustness.

The aforementioned studies primarily focused on the trajectory tracking precision of mobile robots under idealized conditions, relying on a dynamic model that assumed no wheel slippage and overlooked the interaction between the robot's wheels and the ground in practical operational settings. Meanwhile, the existing control methods had problems of low tracking accuracy and insufficient dynamic response ability, making the designed controllers hardly meet the needs of actual operations. Therefore, on the basis of the dynamic relationship analysis between the wheels of high-clearance mobile robots and the ground, this study establishes a kinematic model of wheel slip. At the same time, to achieve fast and high-precision tracking of high-clearance mobile robots, this study uses sliding mode control to design a trajectory tracking controller under two working conditions, improves the system's dynamic response ability through switching gains, and applies a soft switching function to realize a smooth transition of the sliding mode control. This control strategy can further improve the system's tracking performance and provide a reference for the development of high-clearance mobile robot systems.

The remainder of this study is organized as follows. Section 3 delves into the analysis and formulation of the kinematic models for a mobile robot under both slipping and nonslipping conditions, followed by an in-depth design of the soft switching sliding mode control system. Section 4 employs the MATLAB platform to simulate circular trajectory tracking for validation purposes. Section 5 summarizes the findings of this research.

3. Methodology

3.1 Kinematic model of mobile robots

Mobile robots regulate their velocity and directional orientation by varying the speeds of their four independently actuated wheels. The kinematic model of a mobile robot addresses the control challenges related to the robot's speed and positional coordinates. An accurate kinematic model, grounded in geometric principles, delineates the robot's motion characteristics, facilitating rapid tracking of the intended trajectory or pre-planned route. To account for the operational and driving conditions of the mobile robot, redundant rough estimation can be applied to refine the alignment between the robot's state parameters and its kinematic model.

Given the dynamic characteristics of a mobile robot and the complexity of its working environment, if all factors are considered in its kinematic model, the computational load would be considerably large, and real-time performance would be difficult to satisfy. Hence, it is essential to develop a relatively simplified kinematic model for the mobile robot to alleviate computational demands. Concurrently, the overall design and drive configuration of the mobile robot are tailored to meet the requirements of the task at hand. However, a single kinematic model may not accurately reflect the actual operating conditions when characterizing the robot's motion and operational states. Thus, this study uses two different kinematic models of the mobile robot to represent possible changes in its motion state. One is to ignore the wheel slip characteristics caused by the vertical movement of the mobile robot's body to describe the driving state on a hard surface. The other is to consider the wheel slip characteristics of the mobile robot to cover all possible expected driving positions during the operation.

3.1.1 Kinematic model ignoring wheel slip

Assuming that the mobile robot's wheels meet the condition of pure rolling without slipping during the driving process on a hard surface, i.e., the operation condition in which wheel slip is not considered. On the basis of the symmetric structure of the vehicle body, the mobile robot is assumed to exhibit only planar motion in the directions of the *X* and *Y* axes, as well as the yaw around the *Z* axis, ignoring wheel slip. A three-degrees-of-freedom kinematic model of the mobile robot is established, as shown in Fig. 1.

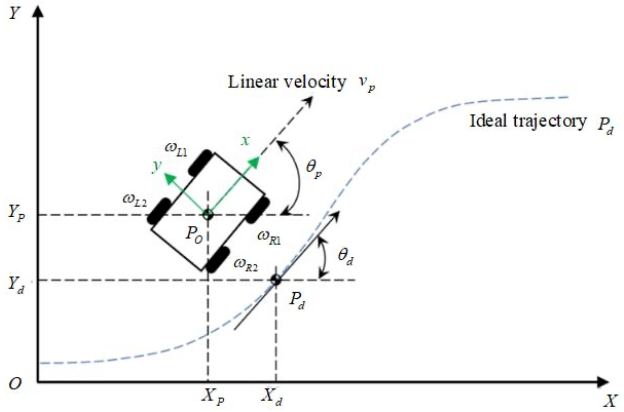

Fig. 1. Motion model of a mobile robot under nonslip condition of wheels

In the motion plane of the mobile robot depicted in Fig. 1, XOY represents the global inertial coordinate system, and XYZ denotes the mobile robot's coordinate system. As the mobile robot moves along the ideal trajectory P_d in two-dimensional space, point P indicates the current position of the mobile robot, which is also the projection of its center of mass onto the inertial coordinate system at point O. The *X*-axis is the projection of the longitudinal symmetry line of the mobile robot's chassis onto the inertial coordinate system XOY, and the *Y*-axis is perpendicular to the *X*-axis at point *O* along the line connecting the centers of the front and rear wheels. In the inertial coordinate system, the desired trajectory and the state of the mobile robot can be represented by the positions of the coordinate system *X* and *Y*, as well as the orientation angle θ. Therefore, $P=(X_p,Y_p,\theta_p)$ represents the global pose of the mobile robot, and ω_{L1}, ω_{L2}, ω_{R1}, and ω_{R2} are the angular velocities of the wheels at the corresponding positions of the mobile robot.

In consideration of the actual driving conditions of the mobile robot, the wheels on the same side can be assumed to have the same angular velocity; hence, $\omega_{L1}=\omega_{L2}=\omega_{L3}$, and $\omega_{R1}=\omega_{R2}=\omega_{R3}$. When the wheel slip condition is ignored, the longitudinal velocity along the direction of travel at the axis center position of each wheel is consistent with the linear velocity of the wheel rotation.

$$V_L=R_c\omega_L, V_R=R_c\omega_R \tag{1}$$

where R_c is the radius of the mobile robot's wheel; V_L and V_R are the longitudinal velocities along the direction of travel on the left and right sides of the mobile robot, respectively.

In the local coordinate system XOY, the linear velocity v_p and angular velocity ω_p of point P in the barycenter position of the mobile robot are represented as follows:

$$\begin{cases} v_p=\dfrac{V_R+V_L}{2}=\dfrac{R_c\omega_R+R_c\omega_L}{2} \\ \omega_p=\dot{\theta}_p=\dfrac{V_R-V_L}{b_w}=\dfrac{R_c\omega_R-R_c\omega_L}{b_w} \end{cases} \tag{2}$$

where b_w is the lateral wheelbase of the mobile robot.

When the wheel slip of the mobile robot is not considered, the lateral displacement *y* and velocity $\dot{y}$ of the wheel in the local coordinate system XOY are both 0; thus, the incomplete constraint conditions of the mobile robot are shown as follows:

$$\dot{Y}_p\cos\theta_p=\dot{X}_p\sin\theta_p \tag{3}$$

Through transformation, Eq. (3) can be expressed in the following vector form:

$$A(q_p)\cdot\dot{q}_p=0 \tag{4}$$

where $A(q_p)=[-\sin\theta_p,\cos\theta_p,0]$.

Introducing a set of bases $S(q_p)$ in zero space $A(q_p)$ satisfies the conditions $A(q_p)\cdot S(q_p)=0$ and $\dot{q}_p=S(q_p)v_p(t)$. Consequently, it is reasonable to disregard the kinematic equations of the mobile robot in global coordinates when considering scenarios where the wheels exhibit longitudinal and lateral slippage. The kinematic equation for the mobile robot in global coordinates, assuming negligible longitudinal and lateral wheel slip, can be derived as follows:

$$\begin{bmatrix}\dot{X}_p\\ \dot{Y}_p\\ \dot{\theta}_p\end{bmatrix}=\begin{bmatrix}\cos\theta_p & 0\\ \sin\theta_p & 0\\ 0 & 1\end{bmatrix}\begin{bmatrix}v_p\\ \omega_p\end{bmatrix} \tag{5}$$

3.1.2 Kinematic model considering wheel slip

During the operation of mobile robots, the loading and harvesting of fruits may cause certain deformation of the tires, while the low-speed rotating wheels of the mobile robot have a high possibility of longitudinal and lateral sliding. Consequently, mobile robots exhibit a constrained state of rolling and sliding during operation. Assuming that the mobile robot only has planar motion in the transverse and longitudinal directions along the *X* and *Y* axes, as well as in the transverse and longitudinal directions around the *Z* axis, and that the wheels on the same side have the same rotational angular velocity, considering wheel slip, the three-degrees-of-freedom kinematic model of the mobile robot is constructed as shown in Fig. 2.

In the motion plane of the mobile robot shown in Fig. 2, *I* is the instantaneous velocity center of the mobile robot, and V_p is the linear velocity of the mobile robot when it is in a slipping state. When the wheels of the mobile robot undergo longitudinal sliding, the longitudinal velocity of the wheel axis is not equal to the linear velocity of the wheel rotation, thus obtaining the longitudinal velocities $V_L^{'}$ and $V_R^{'}$ of the left and right wheel axes when the mobile robot undergoes longitudinal sliding.

$$\begin{cases} V_L' = R_c\omega_L - i_L R_c\omega_L \\ V_R' = R_c\omega_R - i_R R_c\omega_R \end{cases} \tag{6}$$

where i_L and i_R respectively represent the longitudinal slip rates of the left and right wheels of the mobile robot.

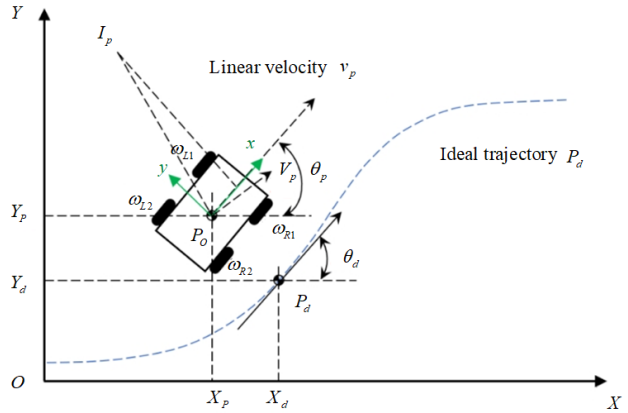

Fig. 2. Motion model of a mobile robot under a wheel slip state

When the mobile robot experiences lateral slip, its linear velocity is not aligned with the *X*-axis along the longitudinal symmetry line of the chassis; instead, a certain lateral slip angle α is present. Consequently, the lateral slip ratio σ of the wheel can be calculated as follows:

$$\sigma = \tan\alpha \tag{7}$$

Fig. 2 and Eq. (2) demonstrate that the linear and angular velocities of the mobile robot's centroid position within the local coordinate system XOY can be articulated as follows:

$$\begin{cases} v_p = \dfrac{V_R' + V_L'}{2} = \dfrac{R_c\omega_R(1-i_R) + R_c\omega_L(1-i_L)}{2} \\ \omega_p = \dot{\theta}_p = \dfrac{V_R' - V_L'}{b_w} = \dfrac{R_c\omega_R(1-i_R) - R_c\omega_L(1-i_L)}{b_w} \end{cases} \tag{8}$$

When the mobile robot undergoes lateral sliding, its lateral velocity in the local coordinate system XOY is expressed as $\dot{y} = \dot{x}\sigma = \dot{x}\tan\alpha$. Accordingly, the kinematic model of the mobile robot in the local coordinate system XOY can be established as follows:

$$\begin{cases} \dot{x} = v_p = \dfrac{R_c\omega_R(1-i_R) + R_c\omega_L(1-i_L)}{2} \\ \dot{y} = \sigma\dot{x} = \sigma\dfrac{R_c\omega_R(1-i_R) + R_c\omega_L(1-i_L)}{2} \\ \omega_p = \dot{\theta}_p = \dfrac{R_c\omega_R(1-i_R) - R_c\omega_L(1-i_L)}{b_w} \end{cases} \tag{9}$$

The transformation relationship between the global and local poses of the mobile robot is delineated as follows:

$$\begin{bmatrix} \dot{X}_p \\ \dot{Y}_p \\ \dot{\theta}_p \end{bmatrix} = \begin{bmatrix} \cos\theta_p & \sin\theta_p & 0 \\ \sin\theta_p & -\cos\theta_p & 0 \\ 0 & 0 & 1 \end{bmatrix} \begin{bmatrix} \dot{x} \\ \dot{y} \\ \dot{\theta}_p \end{bmatrix} \tag{10}$$

Eqs. (8)–(10) show that in consideration of the wheel slip of the mobile robot, its kinematic equation in the global coordinate system XOY is as follows:

$$\begin{bmatrix} \dot{X}_p \\ \dot{Y}_p \\ \dot{\theta}_p \end{bmatrix} = \begin{bmatrix} \cos\theta_p + \sigma\sin\theta_p & 0 \\ \sin\theta_p - \sigma\cos\theta_p & 0 \\ 0 & 1 \end{bmatrix} \begin{bmatrix} v_p \\ \omega_p \end{bmatrix} \tag{11}$$

3.2 Design of a mobile robot controller

Sliding mode variable structure control is implemented in the trajectory tracking control of mobile robots, enabling high-performance tracking capabilities.

3.2.1 Trajectory tracking control under a nonslip condition of wheels

Ignoring the kinematic model of wheel slip (i.e., pure rolling without sliding), the motion trajectory tracking control of the horizontal motion plane of the mobile robot is analyzed as shown in Fig. 1. $P = (X_p, Y_p, \theta_p)$ is the global pose of the mobile robot, and $P_d = (X_d, Y_d, \theta_d)$ is the expected trajectory global pose of the mobile robot. The pose trajectory error equation of the mobile robot can be expressed as follows:

$$e = \begin{bmatrix} X_e \\ Y_e \\ \theta_e \end{bmatrix} = \begin{bmatrix} \cos\theta_p & \sin\theta_p & 0 \\ -\sin\theta_p & \cos\theta_p & 0 \\ 0 & 0 & 1 \end{bmatrix} \begin{bmatrix} X_d - X_p \\ Y_d - Y_p \\ \theta_d - \theta_p \end{bmatrix} \tag{12}$$

The ideal trajectory global pose of the mobile robot satisfies Eq. (5), i.e.,

$$\begin{bmatrix} \dot{X}_d \\ \dot{Y}_d \\ \dot{\theta}_d \end{bmatrix} = \begin{bmatrix} \cos\theta_d & 0 \\ \sin\theta_d & 0 \\ 0 & 1 \end{bmatrix} \begin{bmatrix} v_d \\ \omega_d \end{bmatrix} \tag{13}$$

where v_d and ω_d are the linear and angular velocities of the expected trajectory of the mobile robot, respectively.

The dynamic error equation for the global pose of the mobile robot can be represented as follows by combining Eqs. (12) and (13):

$$\dot{e} = \begin{bmatrix} \dot{X}_e \\ \dot{Y}_e \\ \dot{\theta}_e \end{bmatrix} = \begin{bmatrix} Y_e\omega_p - v_p + v_d\cos\theta_e \\ -X_e\omega_p + v_d\sin\theta_e \\ \omega_d - \omega_p \end{bmatrix} \tag{14}$$

The trajectory tracking problem of the kinematic model of mobile robots is to control the inputs v_p and ω_p such that the pose of the mobile robot can handle any initial error. $\dot{e}$ is bounded, and $\lim_{t\to\infty}\left\|(X_e, Y_e, \theta_e)^T\right\| = 0$.

The sliding surface switching function is taken as follows:

$$s = \begin{bmatrix} s_1 \\ s_2 \end{bmatrix} = \begin{bmatrix} X_e \\ \theta_e + cY_e \end{bmatrix}, c > 0 \tag{15}$$

Then,

$$\dot{s}=\begin{bmatrix}\dot{s}_1\\ \dot{s}_2\end{bmatrix}=\begin{bmatrix}\dot{X}_e\\ \dot{\theta}_e+c\dot{Y}_e\end{bmatrix}=\begin{bmatrix}Y_e\omega_p-v_p+v_d\cos\theta_e\\ \omega_d-\omega_p+c(-X_e\omega_p+v_d\sin\theta_e)\end{bmatrix} \tag{16}$$

Owing to the strip-shaped switching band of the conventional exponential convergence rate in sliding mode variable structure control, it exhibits a chattering phenomenon. A convergence rate with variable speed index is adopted, as shown as follows:

$$\dot{s}=\begin{bmatrix}-\xi_1|s_1|^{\alpha}\operatorname{sgn}(s_1)-k_1s_1|s_1|^{\beta}\\ -\xi_2|s_2|^{\alpha}\operatorname{sgn}(s_2)-k_2s_2|s_2|^{\beta}\end{bmatrix},\quad \xi_1>0,\xi_2>0\ ,k_1>0,k_2>0,\ \alpha>1,0<\beta<1 \tag{17}$$

where $-\xi|s|^{\alpha}\operatorname{sgn}(s)$ can ensure that the system quickly enters the sliding surface, and $-ks|s|^{\beta}$ rapidly approaches the origin within the sliding surface, effectively improving the dynamic quality of the system.

The expression for the control rate can be obtained from Eqs. (16) and (17) as follows:

$$\begin{bmatrix}v_p\\ \omega_p\end{bmatrix}=\begin{bmatrix}\xi_1|s_1|^{\alpha}\operatorname{sgn}(s_1)+k_1s_1|s_1|^{\beta}+Y_e\omega_p+v_d\cos\theta_e\\ \left(\xi_2|s_2|^{\alpha}\operatorname{sgn}(s_2)+k_2s_2|s_2|^{\beta}+\omega_d+cv_d\theta_e\right)\Big/\left(1+cX_e\right)\end{bmatrix} \tag{18}$$

Based on the Lyapunov function $V_s=\frac{1}{2}{s_1}^2+\frac{1}{2}{s_2}^2$,

$$\begin{aligned}\dot{V}_s&=s_1\dot{s}_1+s_2\dot{s}_2\\&=-\xi_1s_1|s_1|^{\alpha}\operatorname{sgn}(s_1)-k_1s_1^2|s_1|^{\beta}-\xi_2s_2|s_2|^{\alpha}\operatorname{sgn}(s_2)-k_2s_2^2|s_2|^{\beta}.\\&=-\xi_1|s_1|^{\alpha+1}-k_1s_1^2|s_1|^{\beta}-\xi_2|s_2|^{\alpha+1}-k_2s_2^2|s_2|^{\beta}\le 0\end{aligned}$$

Therefore, according to Lyapunov stability theory, using the expression of control rate (Eq. [18]), the controlled system (Eq. [14]) of the mobile robot is asymptotically stable. For further weakening the chattering phenomenon, soft switching control is adopted, and its control rate is as follows:

$$\dot{s}=\begin{bmatrix}-\xi_1|s_1|^{\alpha}\tanh(s_1)-k_1s_1|s_1|^{\beta}\\ -\xi_2|s_2|^{\alpha}\tanh(s_2)-k_2s_2|s_2|^{\beta}\end{bmatrix},\quad \xi_1>0,\xi_2>0\ ,k_1>0,k_2>0,\ \alpha>1,0<\beta<1 \tag{19}$$

3.2.2 Trajectory tracking control under a wheel slip condition

The kinematic model accounting for wheel slippage is utilized to analyze the motion trajectory tracking control of the mobile robot during instances of both longitudinal and lateral slippage within the horizontal motion plane. The structural diagram is depicted in Fig. 2, where $P=(X_p,Y_p,\theta_p)$ is the global pose of the mobile robot, and $P_d=(X_d,Y_d,\theta_d)$ is the expected trajectory global pose of the mobile robot. The pose trajectory error equation of the mobile robot in a slip state can be expressed as follows:

$$e=\begin{bmatrix}X_e\\ Y_e\\ \theta_e\end{bmatrix}=\begin{bmatrix}\cos\theta_p+\sigma\sin\theta_p & \sin\theta_p-\sigma\cos\theta_p & 0\\ -\sin\theta_p+\sigma\cos\theta_p & \cos\theta_p+\sigma\sin\theta_p & 0\\ 0 & 0 & 1\end{bmatrix}\begin{bmatrix}X_d-X_p\\ Y_d-Y_p\\ \theta_d-\theta_p\end{bmatrix} \tag{20}$$

The pose trajectory error equation of the mobile robot in a slipping state can be further expressed as follows by combining Eqs. (11) and (20):

$$\dot{e}=\begin{bmatrix}\dot{X}_e\\ \dot{Y}_e\\ \dot{\theta}_e\end{bmatrix}=\begin{bmatrix}Y_e\omega_p-(1+\sigma^2)v_p+(1+\sigma^2)v_d\cos\theta_e\\ -X_e\omega_p+(1+\sigma^2)v_d\sin\theta_e\\ \omega_d-\omega_p\end{bmatrix} \tag{21}$$

The sliding surface switching function is taken as follows:

$$s=\begin{bmatrix}s_1\\ s_2\end{bmatrix}=\begin{bmatrix}X_e\\ \theta_e+cY_e\end{bmatrix},c>0 \tag{22}$$

Then,

$$\dot{s}=\begin{bmatrix}\dot{s}_1\\ \dot{s}_2\end{bmatrix}=\begin{bmatrix}\dot{X}_e\\ \dot{\theta}_e+c\dot{Y}_e\end{bmatrix}=\begin{bmatrix}Y_e\omega_p-(1+\sigma^2)v_p+(1+\sigma^2)v_d\cos\theta_e\\ \omega_d-\omega_p+c\left[-X_e\omega_p+(1+\sigma^2)v_d\sin\theta_e\right]\end{bmatrix} \tag{23}$$

For suppressing the chattering phenomenon, a convergence rate with variable speed index is adopted as follows:

$$\dot{s}=\begin{bmatrix}-\xi_1|s_1|^{\alpha}\operatorname{sgn}(s_1)-k_1s_1|s_1|^{\beta}\\ -\xi_2|s_2|^{\alpha}\operatorname{sgn}(s_2)-k_2s_2|s_2|^{\beta}\end{bmatrix},\quad \xi_1>0,\xi_2>0\ ,k_1>0,k_2>0,\ \alpha>1,0<\beta<1 \tag{24}$$

The expression for the control rate can be obtained from Eqs. (22) and (23) as follows:

$$\begin{bmatrix}v_p\\ \omega_p\end{bmatrix}=\begin{bmatrix}\left[\xi_1|s_1|^{\alpha}\operatorname{sgn}(s_1)+k_1s_1|s_1|^{\beta}+Y_e\omega_p+(1+\sigma^2)v_d\cos\theta_e\right]\Big/(1+\sigma^2)\\ \left[\xi_2|s_2|^{\alpha}\operatorname{sgn}(s_2)+k_2s_2|s_2|^{\beta}+\omega_d+(1+\sigma^2)v_d\sin\theta_e\right]\Big/(1+\sigma^2)\end{bmatrix} \tag{25}$$

According to the Lyapunov function $V_s=\frac{1}{2}{s_1}^2+\frac{1}{2}{s_2}^2$,

$$\begin{aligned}\dot{V}_s&=s_1\dot{s}_1+s_2\dot{s}_2\\&=-\xi_1s_1|s_1|^{\alpha}\operatorname{sgn}(s_1)-k_1s_1^2|s_1|^{\beta}-\xi_2s_2|s_2|^{\alpha}\operatorname{sgn}(s_2)-k_2s_2^2|s_2|^{\beta}\\&=-\xi_1|s_1|^{\alpha+1}-k_1s_1^2|s_1|^{\beta}-\xi_2|s_2|^{\alpha+1}-k_2s_2^2|s_2|^{\beta}\le 0\end{aligned}.$$

Therefore, according to Lyapunov stability theory, using the expression of control rate (Eq. [25]), the controlled system (Eq. [21]) of the mobile robot is asymptotically stable. For further weakening the chattering phenomenon, soft switching control is adopted, and its control rate is as follows:

$$\dot{s}=\begin{bmatrix}-\xi_1|s_1|^{\alpha}\tanh(s_1)-k_1s_1|s_1|^{\beta}\\-\xi_2|s_2|^{\alpha}\tanh(s_2)-k_2s_2|s_2|^{\beta}\end{bmatrix},\quad(26)$$

$$\xi_1>0,\xi_2>0\ ,k_1>0,k_2>0,\ \alpha>1,0<\beta<1$$

4. Result analysis and discussion

Through the MATLAB platform, the dynamic tracking performance of the control strategy is verified in circular trajectory, twisted pair trajectory, and irregular curve trajectory in accordance with the error dynamic model (Eq. [14]) under a nonslip state of the mobile robot wheel in Eq. (19) and the error dynamic model (Eq. [21]) under a nonslip state of the wheel in Eq. (25).

4.1 Trajectory tracking control of mobile robot wheels in a nonslip state

When the mobile robot tracks a circular trajectory, the actual initial pose is $(0.5, 0.5, 45^{\circ})^T$, whereas the ideal initial pose is $(0,1,0^{\circ})^T$. The expected trajectory is ($X_d=\sin t$, $Y_d=\cos t$), the effectiveness of the proposed scheme is verified through MATLAB simulation, and the total simulation time is 30 s. Figs. 3–7 illustrate the lateral position tracking curve, the longitudinal position tracking curve, the directional angle tracking curve, as well as the trajectory tracking and its error curve for the mobile robot during circular trajectory tracking, respectively.

Compared with the results of the simulation without slipping (Figs. 3–7), Figs. 8–13 show the following conclusions under the same initial conditions (the expected horizontal position is $X_d=\sin 0°=0\,m$, whereas the actual position is 0.5 m; the expected horizontal position is $Y_d=\cos 0°=1\,m$, whereas the actual position is 0.5 m): (1) Both states can achieve tracking of the expected position signal and direction angle in a relatively short time within 0.6 s. However, without sliding compensation control (Eq. [20]), significant periodic tracking errors occur in the horizontal and vertical directions, the amplitude reaches 0.065 m (Fig. 12), and the circumferential direction deviates from a fixed-value circle at the center of the expected trajectory (Fig. 11). (2) When sliding occurs, a significant direction angle error exists at the trough of the lateral position, which is due to the sudden change in the corresponding direction angle, equivalent to reversing.

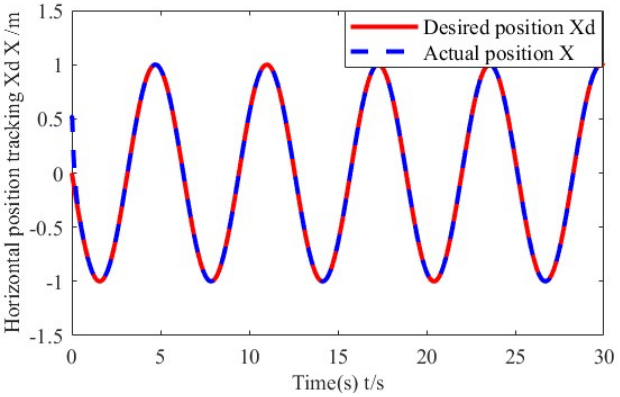

Fig. 3. Horizontal position tracking curve

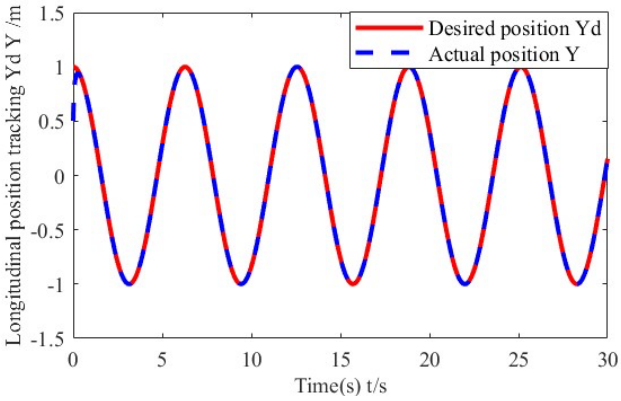

Fig. 4. Longitudinal position tracking curve

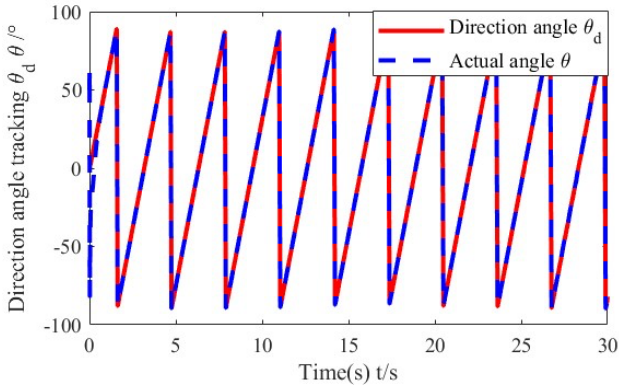

Fig. 5. Direction angle tracking curve

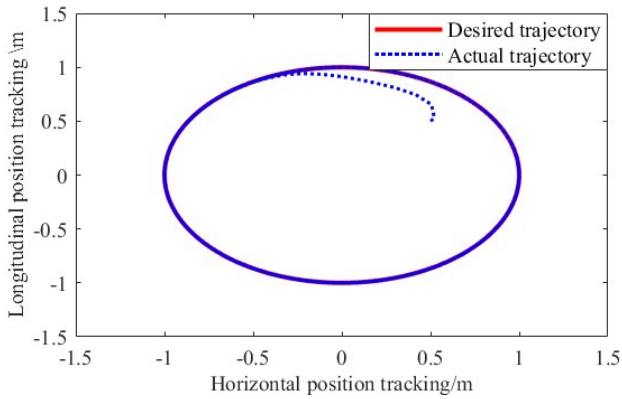

Fig. 6. Circular trajectory tracking curve

Figs. 3 and 4 show that at the initial moment, the expected horizontal position is $X_d=\sin 0°=0\,m$, whereas the actual position is 0.5 m; the expected horizontal position is $Y_d=\cos 0°=1\,m$, whereas the actual position is 0.5 m. These results are consistent with the positions in the figures. The horizontal and vertical positions can achieve tracking of the desired position within 0.6 s, and the tracking error is 0.002 m, as shown in Fig. 7. Fig. 5 illustrates that at the initial moment, the expected direction angle is 0°, whereas the actual direction angle is 45°. Even though the initial directional angle of the mobile robot differs from the intended angle by 45°, the mobile robot can achieve a direction angle tracking error of 1.5° within 0.6 s and 0.05° within 1 s, demonstrating high direction angle tracking accuracy. Fig. 6 shows the circular trajectory tracking curve in the plane. Despite the initial pose of the mobile robot deviating from the expected pose, it is capable of swiftly adjusting to and tracking the anticipated circular trajectory while maintaining a consistent orientation.

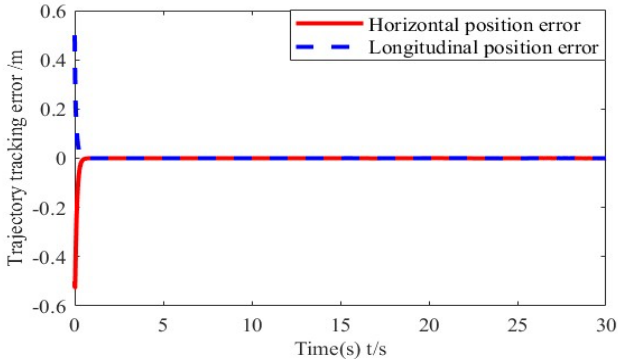

Fig. 7. Circular trajectory tracking error curve

4.2 Trajectory tracking control of mobile robot wheels in a slip state

When the mobile robot tracks a circular trajectory, the actual initial pose is $(0.5, 0.5, 45^{\circ})^T$, whereas the ideal initial pose is $(0, 1, 0^{\circ})^T$. The expected trajectory is ($X_d = \sin t$, $Y_d = \cos t$), and the total simulation time is 30 s. Figs. 8–13 show the lateral position tracking, longitudinal position tracking, direction angle tracking curves, trajectory tracking, and their error curves of the mobile robot without sliding compensation (Eq. [20]) during circular trajectory tracking.

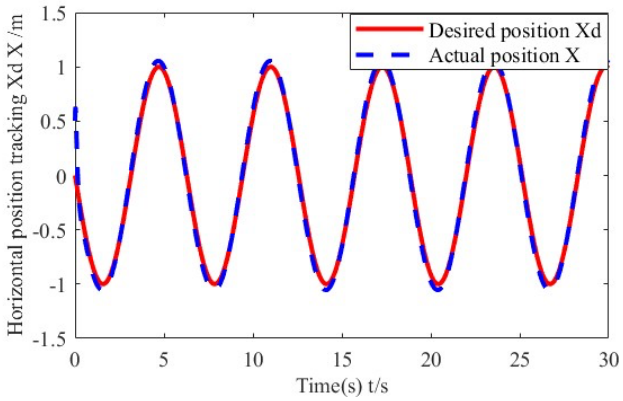

Fig. 8. Horizontal position tracking curve

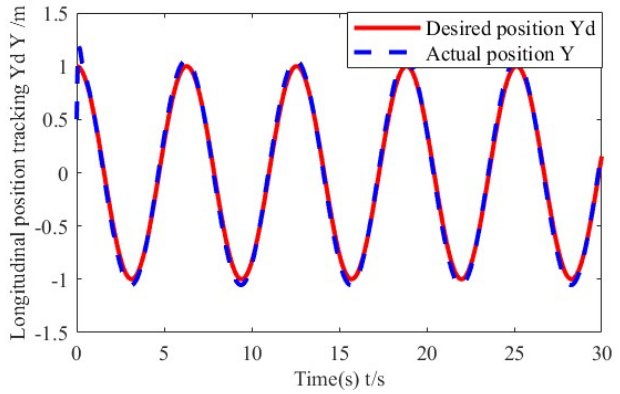

Fig. 9. Longitudinal position tracking curve

Compared with the results of the simulation without slipping (Figs. 3–7), Figs. 8–13 indicate the following conclusions under the same initial conditions (the expected horizontal position is $X_d = \sin 0° = 0\,m$, whereas the actual position is 0.5 m; the expected horizontal position is $Y_d = \cos 0° = 1\,m$, whereas the actual position is 0.5 m): (1) Both states can achieve tracking of the expected position signal and direction angle in a relatively short time within 0.6 s. However, without sliding compensation control (Eq. [20]), significant periodic tracking errors exist in the horizontal and vertical directions, the amplitude reaches 0.065 m (Fig. 12), and the circumferential direction deviates from a fixed-value circle at the center of the expected trajectory (Fig. 11). (2) When sliding occurs, a significant direction angle error exists at the trough of the lateral position, which is due to the sudden change in the corresponding direction angle, equivalent to reversing.

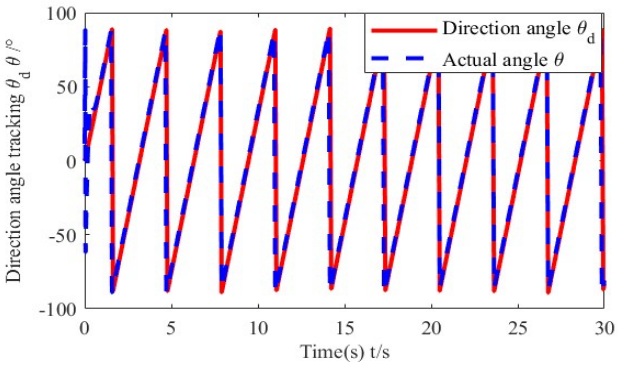

Fig. 10. Direction angle tracking curve

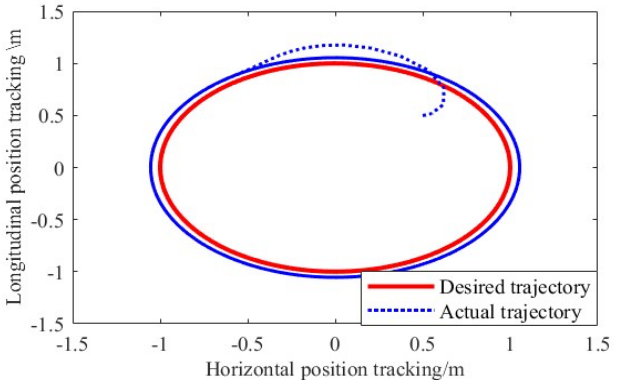

Fig. 11. Circular trajectory tracking curve

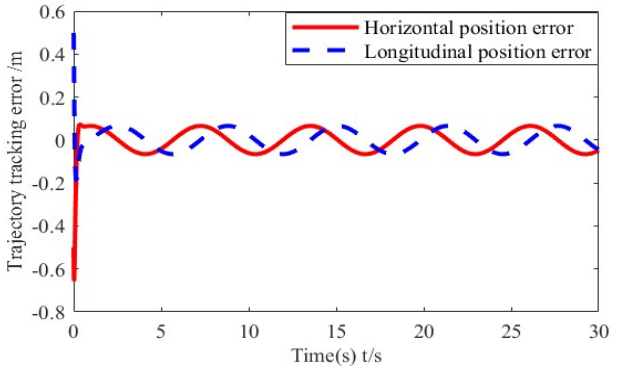

Fig. 12. Trajectory tracking position error curve

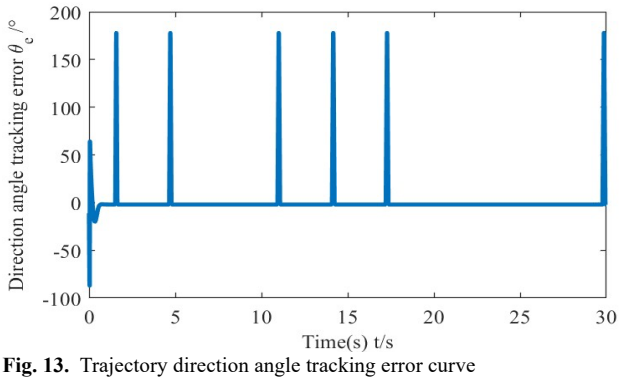

Fig. 13. Trajectory direction angle tracking error curve

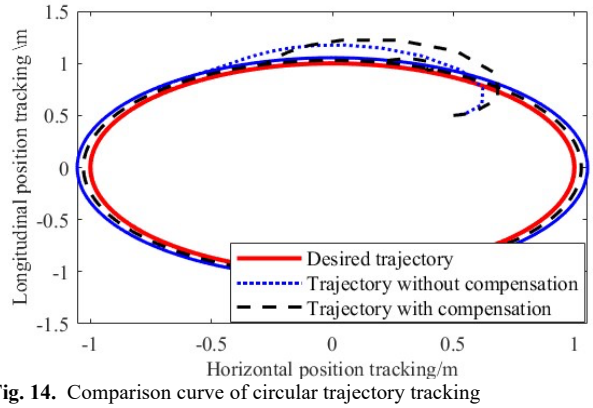

Fig. 14. Comparison curve of circular trajectory tracking

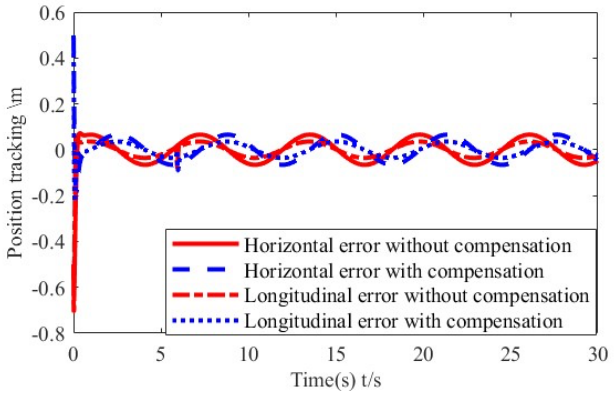

Fig. 15. Comparison curve of circular trajectory tracking error

Figs. 14 and 15 compare the circular trajectory tracking curve and error curve of the mobile robot with and without sliding compensation control (Eq. [26]).

The simulation outcomes presented in Figs. 14 and 15 demonstrate that in the absence of sliding compensation control, the actual trajectory of the mobile robot exhibits a constant deviation from the intended trajectory (with lateral and longitudinal errors of 0.06 m) upon the occurrence of slippage. However, the implementation of sliding compensation can approximately double its precision, with the error being managed to approximately 0.03 m, thereby significantly enhancing the system's tracking accuracy.

5. Conclusion

To address the slippage issue encountered during the operation of high-clearance mobile robots, this study developed a kinematic model for the robots under two distinct operational scenarios: wheel slippage and nonslip conditions. A sliding mode control-based path tracking control strategy for mobile robots was introduced, and the system's tracking performance was evaluated in the context of circular trajectory tracking. The following conclusions could be drawn:

(1) When wheel slip is not considered, the lateral and longitudinal positions can achieve the desired position tracking within 0.6 s, and the tracking error is 0.002 m. Even if the starting direction angle of the mobile robot deviates by 45° from the expected angle, the mobile robot can realize its track direction angles with an error range of 1.5° within 0.6 s and with an error range of 0.05° within 1 s; it can adjust and track the expected circular trajectory in a short time while maintaining consistent pose.

(2) When considering the influence of slip factors, uncompensated sliding mode control generates significant periodic tracking errors in the lateral and longitudinal directions, and its amplitude reaches 0.065 m. The circumferential direction deviates from a fixed-value circle at the center of the expected trajectory, and significant direction angle errors occur at the trough of the lateral position during sliding because of the sudden change in the corresponding direction angle here. The use of sliding compensation can increase its accuracy by about twice, and its error is controlled at around 0.03 m, significantly enhancing the system's tracking precision.

This study considers the actual working conditions of high-altitude-gap mobile robots and establishes a systematic slip dynamic model, making the studied control object highly suitable for actual site conditions and its control performance conform to the actual working conditions. It has certain reference significance for the application and promotion of high-altitude-gap mobile robots in spraying, fertilizing, and other operations. Owing to the lack of actual data on high-altitude-gap mobile robots, in future study, combining actual operational data with the proposed model and making corrections will result in more accurate motion patterns and high-performance control of high-clearance mobile robots in complex operating environments.

Acknowledgements
This work was supported by the Henan Province Science and Technology Development Plan Project of China (Grant Nos. 242102111191 and 242102110333).

References

[1] T. F. Zhuang, X. J. Yang, X. Dong, T. Zhang, H. R. Yan and X. Sun. "Research status and development trend of large self-propelled sprayer booms," *Trans. Chin. Soc. Agr. Mach.*, vol. 49, no. S1, pp. 189-198, Nov. 2018.

[2] J. Du, M. Q. Yu, Y. P. Chen, M. Li, C. Q. Cheng and X. Yin, "Development of an automatic speed control system for high-clearance sprayer," *J. China Agr. Univ.*, vol. 24, no. 12, pp. 104-110, Dec. 2019.

[3] W. Z. Gao, J. D. Zhou, T. Zhou, X. S. Ruan and L. Yang, "Analysis and research on handling stability of plant protection machine based on ADAMS," *J. Agr. Mech. Res.*, vol. 46, no. 1, pp. 35-40, Jan. 2024.

[4] J. Ni, H. P. Mao, L. H. Han, X. D. Zhang, J. Gu and Z. Y. Zuo, "Simulation and test on anti-skid system control for four-wheel drive of high clearance spray machine," *Trans. Chin. Soc. Agr. Mach.*, vol. 41, no. 12, pp. 13-16+21, Dec. 2010.

[5] B. You, L. C. Zhang, Z. Li and L. Ding, "Fuzzy sliding mode trajectory tracking control of wheeled mobile robots," *Comput. Simulat.*, vol. 36, no. 2, pp. 307-313, Feb. 2019.

[6] K. Ding, J. A. Feng, J. Z. Yu and W. B. Wang, "Simulation of roll stability control of high-clearance spray machine," *Comput. Simulat.*, vol. 35, no. 11, pp. 130-134, Nov. 2018.

[7] L. Ding, *et al*, "Longitudinal skid experimental investigation for wheels of planetary exploration rovers," *J. Mech. Eng.*, vol. 51, no. 18, pp. 99-107, Nov. 2015.

[8] T. Nagata and G. Ishigami, "Gyro-based odometry associated with steering characteristics for wheeled mobile robot in rough terrain," *Adv. Robotics*, vol. 30, no. 23, pp. 1495-1508, Dec. 2016.
[9] Z. Sadaf and A. Tauseef, "Performance analysis of path planning algorithms for fruit harvesting robot," *J. Biosyst. Eng.*, vol. 48, no. 2, pp. 178-197, Apr. 2023.
[10] B. Chai, K. Zhang, Mi. H. Tan and J. Y. Wang, "An optimal robust trajectory tracking control strategy for the wheeled mobile robot," *Int. J. Control Autom.*, vol. 22, no. 3, pp. 1050-1065, Jan. 2024.
[11] G. Pandiaraj and S. Muralidharan, "Novel ARC-fuzzy coordinated automatic tracking control of four-wheeled mobile robot," *Intell. Autom. Soft Co.*, vol. 35, no. 3, pp. 3713-3726, Aug. 2023.
[12] G. M. Li, Z. Y. Nie, Z. Y. Li, Y. M. Zheng and J. L. Luo, "Disturbance rejection PID control of wheeled mobile robot under non-equlibrium load," *IET Control Theory A.*, vol. 38, no. 3, pp. 398-406, Jan. 2021.
[13] Y. Y. Xu, Y. Wang, D. B. Xue, "Research on motion error of mobile robot controlled by improved fuzzy neural network PID," *Chin. J. Constr. Mach.*, vol. 17, no. 6, pp. 510-514, Dec. 2019.
[14] R.A. Reza, G. Meysam, T. M. Reza, V. Navid and K. M. Hassan, "A robust intelligent controller-based motion control of a wheeled mobile robot," *Trans. Inst. Meas. Control*, vol. 44, no. 15, pp. 2911-2918, Sep. 2022.
[15] I. Carlucho, M. D. Paula and G. G. Acosta, "An adaptive deep reinforcement learning approach for MIMO PID control of mobile robots," *Int. Soc. Autom. Trans.*, vol. 102, pp. 280-294, Jul. 2020.
[16] Y. J. Zheng, H. Zhao, J. C. Zheng and K. Shao, "Cooperative game-oriented optimal robust control for an uncertain wheeled mobile robot with position constraints," *P. I. Mech. Eng. C-J. MEC.*, vol. 238, no. 10, pp. 4662-4678, May. 2024.
[17] R. M. Colorado, "Observer-based finite-time control for trajectory tracking of wheeled mobile robots with kinematic disturbances," *Int. Soc. Autom. Trans.*, vol. 148, pp. 64-77, Mar. 2024.
[18] H. Ríos, M. Mera, T. Raïssi and Denis Efimov, "Robust interval predictive tracking control for constrained and perturbed unicycle mobile robots," *Int. J. Robust Nonlin.*, vol. 34, no. 9, pp. 6303-6320, Mar. 2024.
[19] E. Hannes, E. Henrik and E. Peter, "Exploration-exploitation-based trajectory tracking of mobile robots using gaussian processes and model predictive control," *Robotic*a, vol. 41, no. 10, pp. 3040-3058, Jun. 2023.
[20] S. Majid, S. S. Jalil and M. Sara, "Trajectory tracking control for mobile robots considering position of mass center," *Optim. Contr. Appl. Met.*, vol. 42, no. 6, pp. 1542-1555, May. 2021.
[21] Z. H. Zhang, X. R. Liu and W. Y. Jiang, "Adaptive tracking control of a nonholonomic wheeled mobile robot with multiple disturbances and input constraints," *At-Autom.*, vol. 72, no. 1, pp. 35-46, Jan. 2024.
[22] Y. Y. Liu, K. Q. Bai, H. Y. Wang and Q. G Fan, "Autonomous planning and robust control for wheeled mobile robot with slippage disturbances based on differential flat," *Inst. Eng. Technol. Control Appl.*, vol. 17, no. 16, pp. 2136-2145, Jul. 2023.
[23] Ho-N. Shou, "Wheeled mobile robot robust control based on hybrid controller approach," *J. Adv. Artif. Life Robot.*, vol. 1, no. 3, pp. 106-111, Jul. 2020.
[24] B. Chai, K. Zhang, M. H. Tan and J. Y. Wang, "An optimal robust trajectory tracking control strategy for the wheeled mobile robot," *Int. J. Control, Autom.*, vol. 22, no. 3, pp. 1050-1065, Jan. 2024.
[25] S. Park and S. M. Lee, "State observer-based physics-informed machine learning for leader-following tracking control of mobile robot," *Int. Soc. Automat. Trans.*, vol. 146, pp. 582-591, Jan. 2024.
[26] P. F. Liu and S. C. Tong, "Fuzzy adaptive fault-tolerant control for underactuated wheeled mobile robot with prescribed performance," *Int. J. Control, Autom.*, vol. 22, no. 6, pp. 1998-2006, May. 2024.
[27] G. C. Onur, "Single-layer neural-network based control of agricultural mobile robot," *Meas. Control*, vol. 56, no. 7-8, pp. 1446-1454, Sep. 2023.
[28] M. Boukens and A. Boukabou, "Design of an intelligent optimal neural network-based tracking controller for nonholonomic mobile robot systems," *Neurocomputing*, vol. 226, pp. 46-57, Jun. 2017.
[29] L. Ovalle, H. Ríos, M. Llama, V. Santibáñez and A. Dzul, "Omnidirectional mobile robot robust tracking: sliding-mode output-based control approaches," *Control Eng. Pract.*, vol. 85, pp. 50-58, Apr. 2019.
[30] A. Alihosseini, N. M. Dehkordi and M. Sajjadi, "Designing a free chattering robust nonlinear sliding mode control for underactuated two wheels mobile robots with disturbances and uncertainties," *J. Vib. Control*, vol. 30, no. 3-4, pp. 685-696, Jan. 2024.